

# Observation of low-field peaks and the temperature evolution of four kinds of magnetization processes in $\text{Pr}_{0.8}\text{Nd}_{0.2}\text{Fe}_{11}\text{Ti}$

T. Zhao, Z. D. Zhang, W. Liu, and X. K. Sun

Shenyang-National Laboratory for Materials Science and International Centre for Materials Physics, Institute of Metal Research, Chinese Academy of Sciences, Wenhua Road 72, Shenyang 110016, People's Republic of China

R. Grössinger

Institute of Experimental Physics, Technical University of Vienna, Wiedner-Hauptstraße 8-10, A-1040, Vienna, Austria

(Received 11 July 2002; revised manuscript received 20 September 2002; published 24 January 2003)

Two abnormal magnetic phenomena, i.e., the low-field peak in the second derivative of magnetization and the temperature evolution of four kinds of magnetization processes in a sequence of Normal→quasi-FOMP→SOMP→FOMP (FOMP and SOMP stand for first- and second-order magnetization processes) are observed experimentally in a compound  $\text{Pr}_{0.8}\text{Nd}_{0.2}\text{Fe}_{11}\text{Ti}$ . An experimental procedure is developed to overcome the difficulty of distinguishing these phenomena. The mechanisms behind these phenomena are also discussed, which are consistent with the predictions of the theoretical calculations of one- and two-sublattice *fixed sample* models based on the mean-field theory. The systematical study of our previous work on the two-sublattice systems is briefly reviewed. A comprehensible description is given of the starting hypothesis, models, and expectations, and conclusions deduced from these experimental data.

DOI: 10.1103/PhysRevB.67.014419

PACS number(s): 75.60.Ej, 75.30.Gw, 75.50.Bb, 75.50.Ww

## I. INTRODUCTION

Understanding magnetic properties of rare-earth transition-metal ( $R$ - $T$ ) intermetallics is very important for developing permanent magnets.<sup>1</sup> The magnetization processes of the  $R$ - $T$  compounds have been investigated systematically by mean-field models, such as the one-sublattice *fixed-sample* model involving anisotropy constants up to the sixth order,<sup>2,3</sup> and the two-sublattice *free-sample* model involving the exchange and the anisotropy constants up to the second order.<sup>2,4</sup> For the *fixed-sample* model, the external field is applied along a certain crystallographic direction so that the Zeeman term is  $M_i B \cos \theta_i$  for each sublattice  $i$ . For the *free-sample* model, the sample is free to rotate in the external magnetic field so that the Zeeman term is  $MB$ , where  $M$  is the vector sum of all sublattice moments  $M_i$ . It is evident that the difference in the Zeeman energy for the *fixed*- and *free-sample* models leads to very much different magnetization processes.

The phase diagrams for the first-order magnetization processes (FOMPs) were given by Asti and Bolzoni for a *fixed-sample* one-sublattice model with three anisotropy constants.<sup>3</sup> In our previous work, it was proved that a FOMP-like jump exists in the magnetization curves even when the set of parameters of the anisotropies is not within FOMP zones, which was defined as a quasi-FOMP.<sup>5,6</sup> The difference is that a FOMP is a first-order transition with a hysteresis loop, whereas a quasi-FOMP is reversible with a very flat energy minimum with respect to the angle  $\theta$  between the moment direction and the  $c$  axis.<sup>5,6</sup> A second-order magnetization process (SOMP) occurs on the borderline between the FOMP and quasi-FOMP zones in the phase diagram.<sup>5</sup> It was expected that the magnetization processes would evolve with decreasing temperature in a sequence of normal→quasi-FOMP→SOMP→FOMP.<sup>5,6</sup>

Some experimental data of fixed samples of well-defined crystallographic axes were shown in Refs. 2 and 4, but no theoretical work on the *fixed-sample* two-sublattice mean-field model, compared with measured  $d^2M/d^2B \sim B$  curves, were given in the reviews.<sup>2,4</sup> In our previous work,<sup>7-9</sup> on the other hand, we studied the magnetization process for a *fixed-sample* two-sublattice mean-field model. A low-field peak was found to emerge in the second derivative of the magnetization with respect to the magnetic field, corresponding to a field-induced noncollinear configuration in two-sublattice ferromagnetic systems, due to the competition among the opposite sublattice anisotropies and the exchange interaction between the sublattice moments.<sup>7,9</sup>

It is interesting to detect whether these two kinds of the abnormal magnetic phenomena exist in the real system to confirm the validity of these theoretical models to the  $R$ - $T$  compounds. In this paper, we report on an experimental observation of the low-field peak and the evolution of the four kinds of magnetization processes in a compound  $\text{Pr}_{0.8}\text{Nd}_{0.2}\text{Fe}_{11}\text{Ti}$ . For a fully comprehensible understanding of these magnetization processes, in Sec. II we first give a theoretical outline of the models, including the *fixed-sample* one-sublattice mean-field model and the *fixed-sample* two-sublattice mean-field model. The different magnetization processes, such as normal, quasi-FOMP, SOMP, FOMP, the low-field peak, etc., are introduced. The systematical study of our previous work on the two-sublattice systems is briefly reviewed. Section III represents the experimental details for the sample preparation, the pulsed field magnetometer, the singular point detection (SPD) technique, etc. The results and discussion are presented in Sec. IV. Section V is for summary.

## II. MODELS

The models employed in this work are based on the mean-field theory. The basic starting hypothesis is that the interac-

tions between magnetic moments are very strong so that they can be treated as a whole to be a sum of the magnetic moments of the same ions/sublattices. The simplest model is the one-sublattice model, in which only the magnetic moments of the ions in one sublattice are taken into account or those of all the ions in several sublattices are treated as a whole. The two-sublattice model takes into account the magnetic moments of two different sublattices, which is much more complicated than the one-sublattice model. The total free energy of a two-sublattice magnet in the presence of an external field is usually expressed as a sum of five terms,

$$E = E_{\text{ex}} + E_{\text{an},A} + E_{\text{an},B} + E_{\text{Zeeman},A} + E_{\text{Zeeman},B} \quad (1)$$

where  $E_{\text{ex}}$  is the energy associated with the exchange interaction between the magnetic moments of the two sublattices,  $E_{\text{an},i}$  ( $i=A,B$ ) is the anisotropy energy for sublattice  $i$  and  $E_{\text{Zeeman},i}$  ( $i=A,B$ ) is the contribution from the interaction between the moment of sublattice  $i$  and the external field.

Either the one-sublattice model or the two-sublattice model can be used for interpreting the experimental results, such as magnetization processes at a certain temperature, the temperature dependence of magnetization, etc., for  $R$ - $T$  intermetallics and also for magnetic thin films or multilayers. Either the one-sublattice model or the two-sublattice model can be dealt within the hypothesis of the *free*- and *fixed-sample* models. The differences between the *free*-model and *fixed-sample* models are as follows: For *free-sample* models the sample is free to rotate in an external magnetic field, while for *fixed-sample* models the external field is applied along a certain crystallographic direction. Therefore, the Zeeman term in the *free-sample* models is  $MB$ , where  $M$  is the vector sum of all sublattice moments  $M_i$ , while the Zeeman term in the *fixed-sample* models is  $M_i B \cos \theta$  for each sublattice  $i$ . In this work, we focus our interests only on the *fixed-sample* models, which will be described in detail separately in Secs. II A and II B for the one- and two-sublattice models.

### A. One-sublattice fixed-sample model

If only one sublattice is magnetic or if the intersublattice exchange is so strong that the moments of the two-sublattice remain collinear during the whole magnetization process, the one-sublattice model is applicable for understanding the magnetic properties of the  $R$ - $T$  compounds or magnetic films. If we neglect the magnetocrystalline anisotropy in the basal plane, the total free energy of a *fixed* uniaxial one-sublattice magnet can be written as

$$E = K_1 \sin^2 \theta + K_2 \sin^4 \theta + K_3 \sin^6 \theta - BM_s \cos(\phi - \theta), \quad (2)$$

where  $\theta$  is the angle between the sublattice magnetic moment  $M_s$  and the  $c$  axis, and  $\phi$  the angle between the direction of the applied magnetic field  $B$  and the  $c$  axis. The magnetocrystalline anisotropy constants are taken into account up to the sixth order  $K_3$ . The magnetization process can be calculated by minimizing  $E$  as a function of  $\theta$  with varying  $B$ ,

$$\begin{aligned} \frac{\partial E}{\partial \theta} &= (K_1 + 2K_2 \sin^2 \theta + 3K_3 \sin^4 \theta) \sin 2\theta - BM_s \sin(\phi - \theta) \\ &= 0 \end{aligned} \quad (3)$$

with the criterion of  $(\partial^2 E / \partial \theta^2) > 0$ .

Then we have

$$B = \frac{(K_1 + 2K_2 \sin^2 \theta + 3K_3 \sin^4 \theta) \sin 2\theta}{M_s \sin(\phi - \theta)} \quad (4)$$

and

$$M = M_s \cos(\phi - \theta) \quad (5)$$

as the set of equations determining the magnetization curve.

The FOMP is a first-order transition during which the magnetic moment irreversibly reorients from an energy minimum to another. During the FOMP, the moment reorientation must overcome an energy barrier that may be equal to the energy maximum between the two-energy minima or to the energy needed for nucleation of a domain in which the magnetic moment has the direction of the second minimum. If the thermal excitation cannot supply enough energy to the magnetic moment to overcome the barrier, a small loop will appear accompanying the FOMP transition in the magnetization curve, which is a common character of the first-order transition. In a one-sublattice magnet, the FOMP can be attributed to the high-order magnetic anisotropy constants. Asti and Bolzoni gave a phase diagram of the FOMPs with respect to the anisotropy constants.<sup>3</sup> According to whether the magnetic moment is directly reoriented into the saturation direction, the FOMPs were classified into two different types.<sup>3</sup> After a type-I FOMP, the magnet reaches the saturation state, otherwise the FOMP is of type II. Thermal evolution of the FOMPs was studied systematically,<sup>10</sup> by an effective parametric method in the mean-field approximation, similar to that used for studying the thermal evolution of the temperature-induced spin reorientation (SR).<sup>11</sup> Phase diagrams for the existence of these thermal behaviors of the FOMPs are given in the anisotropy spaces at zero temperature with the combination of analytical and numerical calculations.<sup>10</sup>

The concept of quasi-FOMPs was introduced in our previous work,<sup>5</sup> which is quite different from that of the FOMPs. The magnetization processes with a FOMP-like anomaly, so-called quasi-FOMPs are reversible processes. During the quasi-FOMP, the energy minima with respect to  $\theta$  become very flat, so that the magnetic moment will rotate substantially upon a slight change in the external field. So the quasi-FOMP is defined as a magnetization process during which there is no discontinuity, and the approach to the saturation proceeds with a point of inflection or a kink. The knee point of the anomalous section in the magnetization curve corresponds to the maximum of moment-rotation rate which appears as a peak in the first derivative of the magnetization curve and as a zero point between two opposite peaks in the second derivative of the magnetization with respect to the external magnetic field.<sup>5,6</sup> This means that the FOMP character would prevail in any system characterized by a set of

anisotropy constants similar to that of FOMP systems, which can exist in the district outside the FOMP's zone in Asti and Bolzoni's phase diagrams.<sup>3,5,6</sup> Similar to the cases of the FOMPs, quasi-FOMPs can be classified into two types I and II. The FOMP-like character of a quasi-FOMP will decrease as the set of the anisotropy constants becomes more different from that favoring a FOMP, and finally it vanishes. The importance of introducing the quasi-FOMPs is evident, due to the following facts: Experimentally, many FOMP-like anomalies have been observed, which do not like the first-order transitions and which are not accompanied by hysteresis loops even at low temperatures. The anisotropy constants for these materials, derived by fitting the magnetization curves, do not indicate a FOMP. Many authors interpreted these anomalies as FOMPs that are rounded by polycrystalline effects or by complicated domain structures even in a single-crystalline sample.

The borderline between a FOMP system and a quasi-FOMP system is a second-order transition (i.e., a SOMP) because the magnetization is continuous but the first derivative has a singular point. In addition, there should exist a normal magnetization process, during which no transition or anomaly is exhibited. So there are four different kinds of magnetization processes: the normal process, the quasi-FOMP, the SOMP, and the FOMP. Figure 1 gives the phase diagrams for these four different magnetization processes.

Because one of the properties of a quasi-FOMP is the existence of a positive section followed by a zero point in the second derivative of the magnetization, the condition for a quasi-FOMP is that the following inequality is satisfied outside the FOMP zone:

$$\frac{d^2M}{dB^2} > 0, \quad \theta \in [\min(\theta_E, \phi), \max(\theta_E, \phi)], \quad (6)$$

where  $\theta_E$  is the angle between the  $c$  axis and the easy magnetization direction, and  $\phi$  the angle between the external field and the  $c$  axis. The condition for a SOMP is one and only one solution of the following equation:

$$\frac{dB}{dM} = 0, \quad \theta \in [\min(\theta_E, \phi), \max(\theta_E, \phi)], \quad (7)$$

If the magnetic field is directed along a symmetry crystal axis, the analytical expressions for the first and second derivatives of the magnetization curve can be derived for the deduction of the quasi-FOMP and SOMP zones from Eqs. (6) and (7). For convenience, we define  $s = \sin \theta$ ,  $c = \cos \theta$ ,  $x = K_2/K_1$ , and  $y = K_3/K_1$ . For  $\phi = 90^\circ$ , Eqs. (4) and (5) take very simple forms (see Ref. 6):

$$\frac{dM}{dB} = \frac{M_s^2}{2K_1(1+6xs^2+15ys^4)}, \quad (8)$$

$$\frac{d^2M}{dB^2} = -\frac{M_s^3s(x+5ys^2)}{4K_1^2(1+6xs^2+15ys^4)}. \quad (9)$$

For  $\phi = 0^\circ$ , one obtains

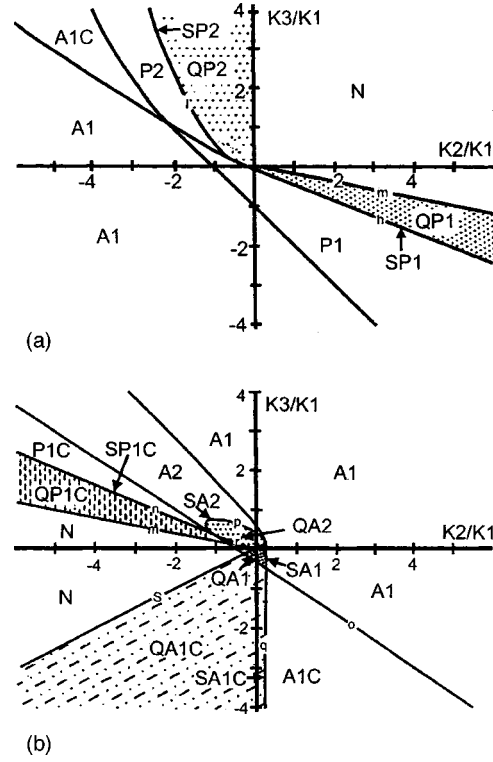


FIG. 1. Phase diagrams for four different magnetization processes: normal, quasi-FOMP, SOMP, and FOMP for (a)  $K_1 > 0$ ,<sup>5</sup> and (b)  $K_1 < 0$ . A1, A2, A1C, P1, P2, and P1C are FOMP zones defined in Ref. 3. QA1, QA2, QA1C, QP1, QP2, and QP1C are the corresponding quasi-FOMP zones, while SA1, SA2, SA1C, SP1, SP2, and SP1C are lines or curves for SOMPs. N is for a normal process. The curves are as follows:  $l: 3x^2 - 5y = 0$ ;  $m: x + 5y = 0$ ;  $n: 1 + 6x + 15y = 0$ ;  $o: 1 + 2x + 3y = 0$ ;  $p: 3(x - 2y)^2 - 5y(1 - 4x) = 0$ ;  $q: 1 - 4x = 0$ ;  $r: x + 3y = 0$ ;  $s: 2x - y = 0$ , with  $x = K_2/K_1$  and  $y = K_3/K_1$ .

$$\frac{dM}{dB} = \frac{M_s^2}{2K_1'(1+6x'c^2+15y'c^4)}, \quad (10)$$

$$\frac{d^2M}{dB^2} = \frac{M_s^3c(x'+5y'c^2)}{4K_1'^2(1+6x'c^2+15y'c^4)}, \quad (11)$$

where  $K_1' = -(K_1 + 2K_2 + 3K_3)$ ,  $K_2' = 2K_2 + 6K_3$ ,  $K_3' = -12K_3$ ,  $x' = K_2'/K_1'$  and  $y' = K_3'/K_1'$ . The quasi-FOMP and SOMP zones obtained by using Eqs. (6)–(11) are shown in Fig. 1, which are labeled with the letters Q and S, respectively. The curves used in Fig. 1 are listed in the figure caption. Similar to the definition in Asti and Bolzoni's phase diagrams,<sup>3</sup> the letters A and P denote the direction of the external field perpendicular and parallel to the  $c$  axis, respectively. The letter C means the easy cone anisotropy of the system. The numbers 1 and 2 correspond to type-I and II quasi-FOMPs, SOMP or FOMPs. The characteristics of a magnetization process depend strongly on the temperature because the high-order anisotropy constants decrease faster than the low-order anisotropy constants. The FOMP, SOMP, and quasi-FOMP, which are caused by the high-order anisotropy constants, will gradually disappear with increasing tem-

perature. At high temperature, like room temperature, only the normal magnetization process is likely to show up. It was predicted that the magnetization processes would evolve with decreasing temperature in a sequence of normal  $\rightarrow$  quasi-FOMPs  $\rightarrow$  SOMPs  $\rightarrow$  FOMPs.<sup>5,6</sup>

### B. Two-sublattice fixed-sample model

For a *fixed* single crystal with two magnetic sublattices, the total free energy can be expressed as

$$E = n_{AB} M_A M_B \cos(\theta_A - \theta_B) + \sum_{i=1}^3 \sum_{j=A,B} K_{ij} \sin^{2i} \theta_j - \sum_{j=A,B} B M_j \cos(\phi - \theta_j), \quad (12)$$

where the exchange energy between the two magnetic sublattices, the anisotropy energies up to the sixth-order anisotropy constant  $K_{3A}$  (or  $K_{3B}$ ), and the Zeeman energies of the magnetic moments  $M_j$  ( $j=A, B$ ) of each sublattice are taken into account.  $\theta_A$  (or  $\theta_B$ ) is the angle between the sublattice magnetic moments  $M_A$  (or  $M_B$ ) and the  $c$  axis, and  $\phi$  the angle between the direction of the applied magnetic field  $B$  and the  $c$  axis. So the configuration of the moments of the sublattices is determined by these energies. At equilibrium, one has

$$\frac{\partial E}{\partial \theta_A} = n_{AB} M_A M_B \sin(\theta_B - \theta_A) + \sum_{i=1}^3 i K_{iA} \sin^{2i-2} \theta_A \sin 2\theta_A - B M_A \sin(\phi - \theta_A) = 0, \quad (13)$$

$$\frac{\partial E}{\partial \theta_B} = n_{AB} M_A M_B \sin(\theta_A - \theta_B) + \sum_{i=1}^3 i K_{iB} \sin^{2i-2} \theta_B \sin 2\theta_B - B M_B \sin(\phi - \theta_B) = 0 \quad (14)$$

with the criterion of

$$\Delta = \left( \frac{\partial^2 E}{\partial \theta_A \partial \theta_B} \right)^2 - \frac{\partial^2 E}{\partial \theta_A^2} \frac{\partial^2 E}{\partial \theta_B^2} < 0; \frac{\partial^2 E}{\partial \theta_A^2} > 0; \frac{\partial^2 E}{\partial \theta_B^2} > 0.$$

The magnetization processes of a two-sublattice magnet are profuse, because a bending of the magnetic moments could occur, accompanying their noncollinear configurations, when the external field is applied. A study of spin configurations in a two-sublattice system revealed that noncollinear spin configurations exist even in the absence of an external field, which originate from the competition among the exchange interaction and the opposite magnetic anisotropies of the two sublattices.<sup>12</sup> The phase diagrams were given for different spin configurations at the zero field of the two-sublattice system, which were derived by considering the anisotropy constants up to the second (or sixth) order.<sup>12</sup> When the magnetic field is applied, the magnetization processes are determined by the total free energy of Eq. (12) as well as the equilibrium condition of Eqs. (13) and (14). A computation procedure was developed to calculate not only the magnetization curve but also the first and second deriva-

tives of the magnetization with respect to the magnetic field of the two-sublattice ferromagnet.<sup>7</sup> It was found that, besides the peaks in the high-field range corresponding to the anisotropy field, a low-field peak could emerge in the second-order derivative curves of magnetization, depending sensitively on the competition between the exchange energy and the high competing single-ion anisotropies of the two-sublattice system.<sup>7,9,13,14</sup> The effects of the exchange interaction and the anisotropies were discussed,<sup>9</sup> and the phase diagrams for the existence of the low field peaks were given.<sup>14</sup> The existence of a low-field peak is a characteristic of the two-sublattice system, which has not been detected experimentally up to date, to our knowledge. It was clear that only the second-order competing anisotropies of the two sublattices are needed for prediction of the low-field peak.<sup>7,9,13,14</sup> If the high-order anisotropies were taken into account, the FOMPs would occur at the high-field range of the magnetization curve.<sup>6</sup> Of course, the situation becomes much more complex in the two-sublattice system. The bending processes occur so that the magnetic moments of the two sublattices could jump either together or separately; thus more than one FOMP could occur in one magnetization curve.<sup>6</sup> For comparison between the *fixed-sample* and the *free-sample* models, the readers can refer to the literature for the study of the magnetization processes in a two-sublattice *free-sample* system.<sup>2,4,15</sup>

The temperature dependence of the magnetization of the two-sublattice system was investigated systematically.<sup>16-19</sup> Some phenomena, including the ferrimagneticlike anomaly in a two-sublattice ferromagnet,<sup>16</sup> the first-order spin reorientation reform,<sup>17</sup> and the second-order spin reorientation reform<sup>18,19</sup> were predicted in a certain condition for the temperature dependence of the spontaneous magnetization in the two-sublattice system.

### III. EXPERIMENTAL DETAILS

The SPD technique developed by Asti and Rinaldi is a convenient method to determine the anisotropy field and the FOMP transition field of polycrystalline samples.<sup>20,21</sup> Due to the noise signal at low field range of the SPD, it is usually hard to pick the low-field peak out of the background. The problem is not only to search which compound exhibits this kind of phenomenon in its SPD curve, but also to confirm that the peak really belongs to the intrinsic behaviors of the compound. On the other hand, more difficulty arose in distinguishing a quasi-FOMP from a FOMP experimentally (there is much more difficulty in the case of polycrystalline samples). In this work, we develop a procedure to overcome this difficulty to illustrate the temperature evolution of the four kinds of magnetization processes.

A polycrystalline compound  $\text{Pr}_{0.8}\text{Nd}_{0.2}\text{Fe}_{11}\text{Ti}$  was prepared by arc melting.<sup>22</sup> The homogenized ingot, after being annealed at 1100 °C for 15 days, is essentially of single phase with a tetragonal  $\text{ThMn}_{12}$ -type structure. Some magnetic phase transitions in this compound were studied in a previous report.<sup>22</sup> Measurements of the anisotropy field  $B_a$ , the critical fields  $B_{c0}$  of a FOMP (or SOMP or quasi-FOMP), and the fields  $B_{\text{low}}$  of the low-field peak for an aligned

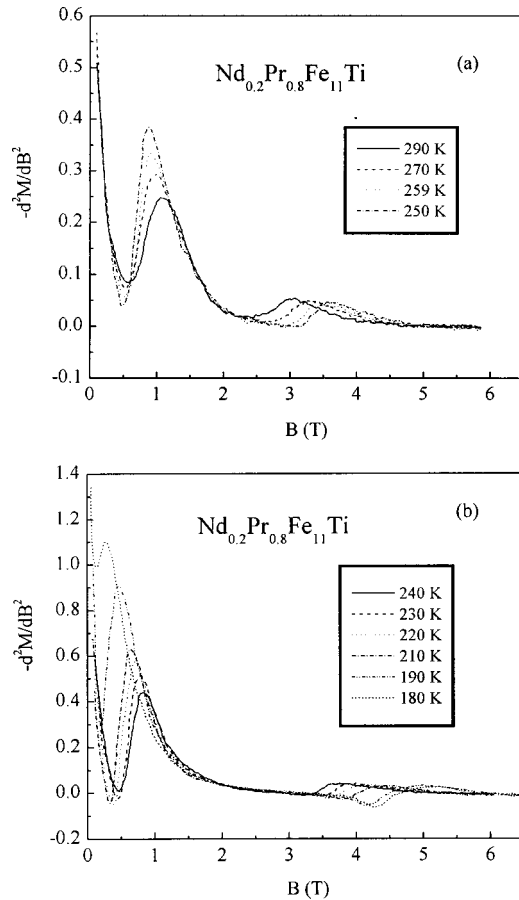


FIG. 2. SPD curves at different temperatures for  $\text{Pr}_{0.8}\text{Nd}_{0.2}\text{Fe}_{11}\text{Ti}$

$\text{Pr}_{0.8}\text{Nd}_{0.2}\text{Fe}_{11}\text{Ti}$  sample were carried out by means of the SPD technique in the pulsed-field facilities at the Institute for Experimental Physics, Technical University of Vienna, operated from 4.2–300 K with a maximum field of 30 T. In a uniaxial magnetic compound, a singularity in  $d^2M/d^2B \sim B$  occurs at  $B = B_a$ , with the field perpendicular to the alignment direction of the sample. For a sample with an easy plane magnetization, like  $\text{Pr}_{0.8}\text{Nd}_{0.2}\text{Fe}_{11}\text{Ti}$ , a cylindrical sample was prepared by the rotation-alignment method aligning powders in a field of 1 T and fixing them in epoxy resin.<sup>22,23</sup> The magnetic field was applied along the direction perpendicular to the alignment direction.

#### IV. RESULTS AND DISCUSSION

SPD curves of the magnetization measured at 180–290 K are given in Figs. 2(a) and 2(b) for  $\text{Pr}_{0.8}\text{Nd}_{0.2}\text{Fe}_{11}\text{Ti}$ . Besides the peaks in the high-field range corresponding to the anisotropy fields, clear low-field peaks are found on the SPD curves from room temperature to 200 K. The signal of the low-field peaks is much pronounced than the background, and thus cannot be due to the noise signal. The decrease of  $B_{\text{low}}$  with decreasing temperature distinguishes it clearly from that of the coercivity. The shift of the low-field peak positions, depending on the temperature, is attributed to the text that the strength of the exchange coupling between the

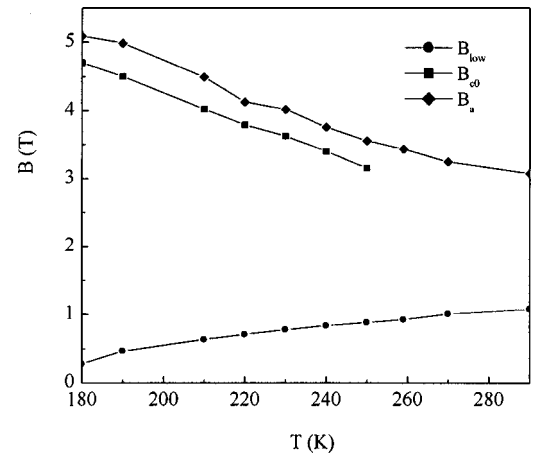


FIG. 3. Temperature dependence of the anisotropy field  $B_a$ , the critical field  $B_{c0}$  of a quasi-FOMP or a SOMP or FOMP, and the field  $B_{\text{low}}$  of the low-field peaks for  $\text{Pr}_{0.8}\text{Nd}_{0.2}\text{Fe}_{11}\text{Ti}$ .

sublattice moments is comparable with the competing anisotropies of the two sublattices.<sup>7,9</sup> Figure 3 shows the temperature dependence of the anisotropy fields  $B_a$  and the fields  $B_{\text{low}}$  of the low-field peaks.  $B_a$  increases from 3.08 to 5.09 T, while  $B_{\text{low}}$  decreases from 1.08 to 0.27 T when the temperature is from 290 to 180 K. There is a clear concave point at about 220 K in the curve for the anisotropy field  $B_a$ , showing the occurrence of some anomalies in the SPD curve.

According to our theory of a quasi-FOMP,<sup>5,6</sup> its critical field was identified as the field at which the SPD curve cross zero ( $B_{c0}$ ). A quasi-FOMP temperature  $T_{\text{quasi-FOMP}}$  was identified where double peaks appear at the SPD curve and, the SPD curve begins to cross zero (for onset of a quasi-FOMP, not of a FOMP, as stated in Asti and Rinaldi's work<sup>20,21</sup>). From Fig. 2(a), we have  $T_{\text{quasi-FOMP}} = 250$  K. Figure 3 shows that  $B_{c0}$  increases from 3.16 to 4.70 T when the temperature decreases from 250 to 180 K. The question is how to identify the temperature for the onset of a FOMP. By a theoretical prediction,<sup>24</sup> we expect that at the onset temperature  $T_{\text{FOMP}}$  there exists a singularity on the temperature dependence of  $B_{c0}$  because actually a SOMP occurs at this temperature (so better to call it  $T_{\text{SOMP}}$ ).<sup>24</sup> A concave point exists in the curve in Fig. 3 for the critical field  $B_{c0}$ , accompanying that for the anisotropy field  $B_a$ . The singularity can be seen more clearly on the  $dB_{c0}/dT - T$  plot in Fig. 4(a). The experimental data are first smoothed as in Fig. 4(b), and then the derivative is done by a built-in function of the commercial ORIGIN 5.0 software.<sup>25</sup> We have successfully found  $T_{\text{SOMP}} = 225$  K, which is about 25 K lower than  $T_{\text{quasi-FOMP}}$ . Therefore, the temperature evolution of the four kinds of magnetization processes has been observed in a sequence of normal  $\rightarrow$  quasi-FOMP  $\rightarrow$  SOMP  $\rightarrow$  FOMP, in good agreement with our theoretical prediction.<sup>5,6</sup>

The phase diagrams of these four magnetization processes are given in Figs. 1(a) and 1(b) for  $K_1 > 0$ ,<sup>5</sup> and  $K_1 < 0$ , respectively. The present compound with an easy plane anisotropy corresponds to the phase diagram in Fig. 1(b) for  $K_1 < 0$ . During a quasi-FOMP, the knee point of the anomalous section in the magnetization curve corresponds to the maximum of moment-rotation rate, appearing as a peak in its first

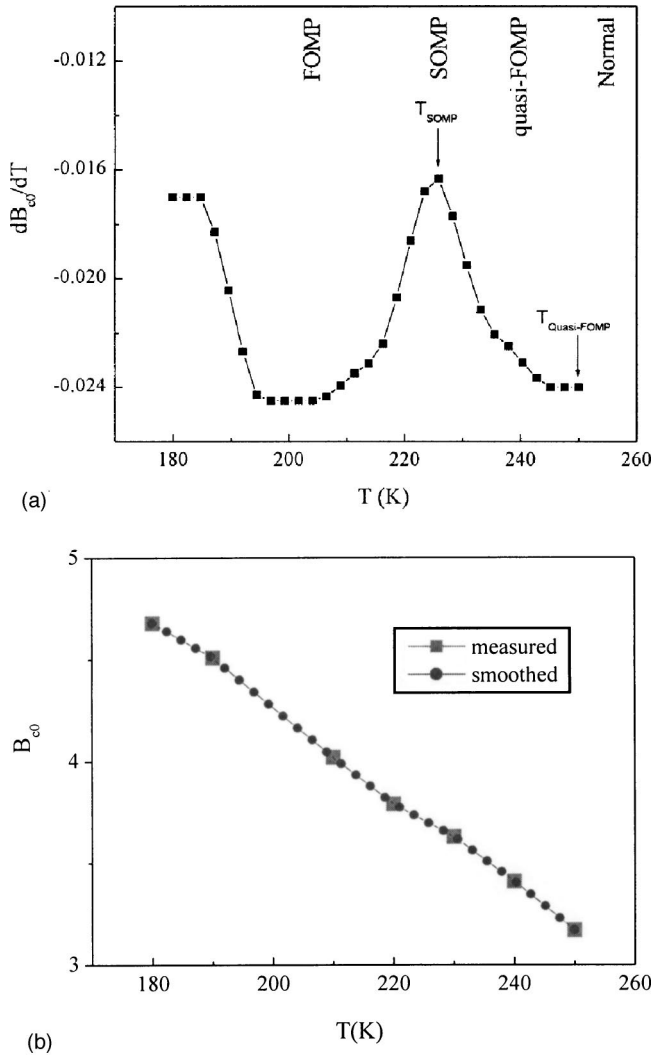


FIG. 4. (a)  $dB_{c0}/dT$  vs the  $T$  plot for  $\text{Pr}_{0.8}\text{Nd}_{0.2}\text{Fe}_{11}\text{Ti}$ . (b) shows the experimental data and the smoothed curves.

derivative and as a zero point between two opposite peaks in its second derivative of the magnetization with respect to the magnetic field. As mentioned above in Sec. II A, the condition for a quasi-FOMP is that the inequality of  $d^2M/dB^2 > 0$  is satisfied outside the FOMP zone in Asti and Bolzoni's FOMP phase diagram.<sup>3</sup> The condition of  $dB/dM=0$  is for an infinite discontinuity in the first derivative of the magnetization during a SOMP,<sup>5,6,24</sup> located at the borderline between the FOMP and quasi-FOMP zones. An example of calculations, illustrated in Fig. 5(a), shows the existence of even a stronger singularity on the  $B_{c0}-T$  plot. The peak at  $T=0.58T_c$  corresponds to the SOMP, when the ratios for the anisotropy constants  $K_2/K_1$  and  $K_3/K_1$  cross the curve  $p$  in the phase diagram Fig. 1(b). Zener's power laws were used for deducing temperature dependence of the anisotropy coefficients  $\kappa_2$ ,  $\kappa_4$ , and  $\kappa_6$  [see Fig. 5(b)].<sup>26</sup> The concave point for the critical field  $B_{c0}$  in Fig. 3 can also be reproduced by adjusting the anisotropy parameters. However, it is difficult to analyze the experimental data quantitatively by our two-sublattice mean-field model, not only because the polycrystalline character of the present sample, but also because of

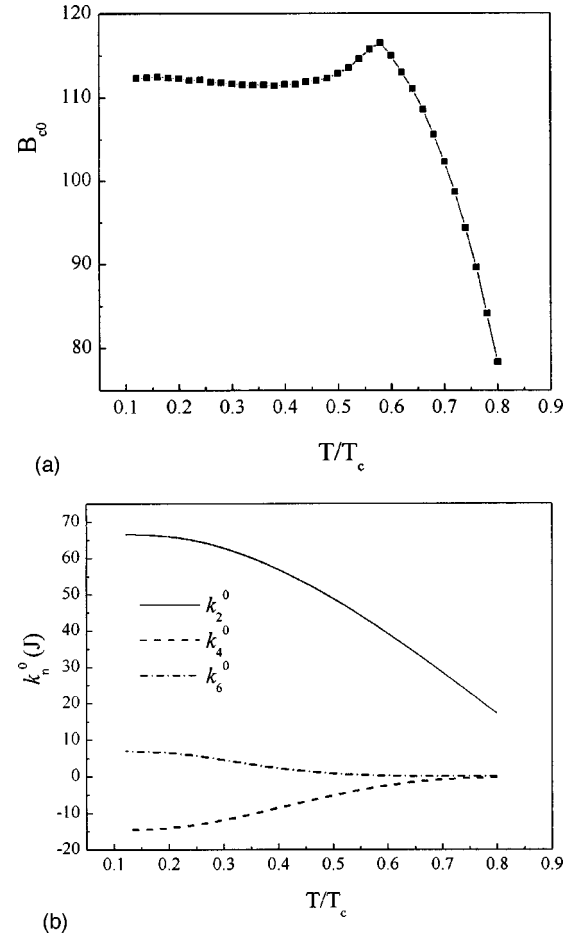


FIG. 5. (a)  $B_{c0}$  vs the  $T$  plot calculated based the Zener's power law.  $B_{c0}$  corresponds to the maximum value of  $dM/dB$  for each temperature. (b) shows the temperature dependence of the anisotropy coefficients  $\kappa_2^0$ ,  $\kappa_4^0$ , and  $\kappa_6^0$ . The parameters used during the calculations are  $J=2$ ,  $M(0)=1$ ,  $K_1=-100$  J,  $K_2=100$  J, and  $K_3=-100$  J.

weaknesses of the pulse field measurement, such as the noisy data.<sup>25</sup> The difficulties are also due to the sensitivity of the second-order derivative of the magnetization, which depends strongly on the magnetic parameters, such as the exchange constant, the anisotropy constants of the two sublattices, etc., Nevertheless, more experimental data recorded on a single crystal would be quite helpful.

The present work is consistent with our theoretical predictions, based on the one- and two-sublattice *fixed-sample* models. The one-sublattice model is the simplest one, for analytical solutions can be easily derived to give the phase diagrams for the different magnetization processes.<sup>3,5,6</sup> The existence of the low-field peaks is part of the character of a two-sublattice *fixed-sample* system, suggesting that a two-sublattice model is needed for describing quantitatively the whole magnetization process of the present compound.<sup>7,9</sup> However, it is hard to derive the analytical solution in the presence of fields for two-sublattice systems to give the phase diagrams for the magnetization processes (like FOMPs) at the high-field range. Nevertheless, the phase diagram for FOMPs, quasi-FOMPs, and SOMPs, derived based

on the one-sublattice model, is still useful for illustrating these phenomena qualitatively. This is because for *fixed samples*, competition between the two sublattices, such as bending of the moments, mainly occurs at the low-field range where the low-field peaks emerge,<sup>7,9</sup> while the character of the system can be treated approximately by the one-sublattice *fixed-sample* model in the high-field range where the FOMPs, quasi-FOMPs, or SOMP usually occur.

The present work indicates that the one and two-sublattice mean-field models are valid to a certain extent for interpreting the magnetic properties and for predicting the phenomena of the *R-T* intermetallics. Furthermore, the one- and the two-sublattice mean-field models are applicable for interpreting the experimental results in magnetic thin films.<sup>27-30</sup>

## V. SUMMARY

In summary, the systematical study of our previous work on two-sublattice systems has been briefly reviewed. A comprehensible description has been given of the starting hypothesis, models, expectations, and conclusions deduced

from the experimental data. We have observed low-field peaks in the second derivative of the magnetization and the temperature evolution of four kinds of magnetization processes (normal→quasi-FOMP→SOMP→FOMP), by employing the SPD technique. Because the second derivative of the magnetization corresponds to the acceleration of the moment rotation, studying the low-field peaks as well as the four magnetization processes in detail provides us with deeper insight into the magnetic behaviors of the materials. The experimental findings in this work indicate that the one- and two-sublattice mean-field models are valid to a certain extent for interpreting the magnetic properties and for predicting the phenomena of the *R-T* intermetallics.

## ACKNOWLEDGMENTS

This work was supported by Project Nos. 59725103 and 10274087 of the National Natural Science Foundation of China, and by the Science and Technology Commission of Shenyang.

- 
- <sup>1</sup>J. F. Herbst, *Rev. Mod. Phys.* **63**, 819 (1991).  
<sup>2</sup>J. J. M. Franse and R. J. Radwański, in *Rare-Earth Iron Permanent Magnets*, edited by J. M. D. Coey (Oxford University Press, New York, 1996), pp. 58–158.  
<sup>3</sup>S. Asti and F. Bolzoni, *J. Magn. Magn. Mater.* **20**, 29 (1980).  
<sup>4</sup>J. J. M. Franse and R. J. Radwański, in *Handbook of Magnetic Materials*, edited by K. H. J. Buschow (Elsevier, Amsterdam, 1993), Vol. 7, pp. 307–501.  
<sup>5</sup>T. Zhao, X. K. Sun, Z. D. Zhang, Q. Wang, Y. C. Chuang, and F. R. de Boer, *J. Magn. Magn. Mater.* **104–107**, 2119 (1992).  
<sup>6</sup>T. Zhao, Ph.D thesis, Shenyang-Amsterdam, 1995.  
<sup>7</sup>Z. D. Zhang, T. Zhao, X. K. Sun, and Y. C. Chuang, *J. Appl. Phys.* **71**, 3434 (1992).  
<sup>8</sup>An error is found in Eq. (9) of Ref. 7, which was due to a mistyping and should be revised as
- $$dF = \left( \frac{\partial F}{\partial \theta_A} + \frac{\partial F}{\partial \theta_B} \times W \right) d\theta_A.$$
- “cos” in the denominators of Eqs. (3a) and (3b) of Ref. 7 should be corrected to “sin.”  
<sup>9</sup>Z. D. Zhang, T. Zhao, D. Y. Geng, X. K. Sun, and Y. C. Chuang, *Phys. Status Solidi A* **134**, 201 (1992).  
<sup>10</sup>M. H. Yu, Z. D. Zhang, F. R. de Boer, E. Brück, and K. H. J. Buschow, *Phys. Rev. B* **65**, 104414 (2002).  
<sup>11</sup>M. H. Yu and Z. D. Zhang, *Phys. Rev. B* **60**, 12 107 (1999).  
<sup>12</sup>Z. D. Zhang, T. Zhao, F. R. de Boer, and P. F. de Châtel, *J. Magn. Magn. Mater.* **147**, 74 (1995).  
<sup>13</sup>T. Zhao, Z. D. Zhang, X. K. Sun, and Y. C. Chuang, *J. Magn. Magn. Mater.* **117**, 387 (1992).  
<sup>14</sup>Z. D. Zhang, T. Zhao, D. Y. Geng, X. K. Sun, and Y. C. Chuang, *Phys. Status Solidi A* **134**, 475 (1992).  
<sup>15</sup>Z. D. Zhang, T. Zhao, F. R. de Boer, and P. F. de Châtel, *J. Magn. Magn. Mater.* **174**, 269 (1997).  
<sup>16</sup>Z. D. Zhang, M. H. Yu, and T. Zhao, *J. Magn. Magn. Mater.* **174**, 261 (1997).  
<sup>17</sup>M. H. Yu, T. Zhao, and Z. D. Zhang, *Phys. Status Solidi A* **164**, 827 (1997).  
<sup>18</sup>M. H. Yu and Z. D. Zhang, *J. Magn. Magn. Mater.* **232**, 60 (2001).  
<sup>19</sup>M. H. Yu, T. Zhao, and Z. D. Zhang, *J. Magn. Magn. Mater.* **246**, 310 (2002).  
<sup>20</sup>G. Asti and S. Rinaldi, *Phys. Rev. Lett.* **28**, 1584 (1972).  
<sup>21</sup>G. Asti and S. Rinaldi, *J. Appl. Phys.* **45**, 3600 (1974).  
<sup>22</sup>W. Liu, X. K. Sun, Z. D. Zhang, J. L. Wang, T. Zhao, Q. F. Xiao, E. Brück, F. R. de Boer, and R. Grössinger, *J. Phys.: Condens. Matter* **10**, 379 (1998).  
<sup>23</sup>Q. Wang, Z. G. Zhao, W. Liu, X. K. Sun, and Y. C. Chuang, *J. Magn. Magn. Mater.* **109**, 59 (1992).  
<sup>24</sup>The condition of  $dB/dM=0$ , i.e.,  $dM/dB \rightarrow \infty$ , exists at the critical point  $B_{c0}$  for a SOMP transition. The singularity of the susceptibility at that  $B_{c0}$  could be equalized to a singularity in the  $B_{c0} \sim T$  curve for a FOMP, a SOMP, and a quasi-FOMP.  
<sup>25</sup>The data points derived from the pulse field measurement are usually noisy. A small fluctuation in the neighboring points on the original curve can be amplified into noise peaks in the derivative curve, which is large enough to bury the real trend. Meanwhile, we cannot get enough data points at present (because of the temperature control limit) to get a good derivative. As we understand, doing a smooth point first and then doing a derivative point is a rather general practice to deal with this kind of problem. Nevertheless, more experimental data recorded on a single crystal would be quite helpful for removing the speculation at this point.  
<sup>26</sup>C. Zener, *Phys. Rev.* **96**, 1335 (1954).  
<sup>27</sup>M. H. Yu, Z. D. Zhang, and T. Zhao, *J. Magn. Magn. Mater.* **195**, 327 (1999).  
<sup>28</sup>M. H. Yu and Z. D. Zhang, *J. Magn. Magn. Mater.* **195**, 515 (1999).  
<sup>29</sup>G. Wiatrowski, *J. Magn. Magn. Mater.* **212**, 29 (2000).  
<sup>30</sup>S. M. Valvidares, L. M. Alvarez-Prado, J. I. Martin, and J. M. Alameda, *Phys. Rev. B* **64**, 134423 (2001).